European Journal of Pharmaceutical Sciences 136 (2019) 104943

Contents lists available at ScienceDirect

European Journal of Pharmaceutical Sciences

journal homepage: www.elsevier.com/locate/ejps

Predicting pharmacokinetic behaviour of drug release from drug-eluting embolization beads using *in vitro* elution methods

Alice Hagan[a,b,1], Marcus Caine[b,1], Cara Press[b], Wendy M. Macfarlane[a], Gary Phillips[a], Andrew W. Lloyd[a], Peter Czuczman[b], Hugh Kilpatrick[b,1], Zainab Bascal[b,1], Yiqing Tang[b,1], Pedro Garcia[b], Andrew L. Lewis[b,*,1]

[a] School of Pharmacy and Biomolecular Sciences, University of Brighton, Moulsecoomb, Brighton BN2 4GJ, UK
[b] Biocompatibles UK Ltd, a BTG International Group Company, Lakeview, Riverside Way, Watchmoor Park, Camberley, GU15 3YL, UK

ARTICLE INFO

Keywords:
IVIVC
Drug-eluting beads
Chemoembolisation
Vandetanib
Drug delivery

ABSTRACT

Drug-eluting Embolic Bead - Transarterial Chemoembolisation (DEB-TACE) is a minimally invasive embolising treatment for liver tumours that allows local release of chemotherapeutic drugs *via* ion exchange, following delivery into hepatic arterial vasculature. Thus far, no single *in vitro* model has been able to accurately predict the complete kinetics of drug release from DEB, due to heterogeneity of rate-controlling mechanisms throughout the process of DEB delivery. In this study, we describe two *in vitro* models capable of distinguishing between early phase and late phase drug release by mimicking *in vivo* features of each phase. First, a vascular flow system (VFS) was used to simulate the early phase by delivering DEB into a silicon vascular cast under high pulsatile flow. This yielded a burst release profile of drugs from DEB which related to the dose adjusted C_{max} observed in pharmacokinetic plasma profiles from a preclinical swine model. Second, an open loop flow-through cell system was used to model late phase drug release by packing beads in a column with an ultra-low flow rate. DEB loaded with doxorubicin, irinotecan and vandetanib showed differential drug release rates due to their varying chemical properties and unique drug-bead interactions. Using more representative *in vitro* models to map discrete phases of DEB drug release will provide a better capability to predict the pharmacokinetics of developmental formulations, which has implications for treatment safety and efficacy.

1. Introduction

Drug-Eluting embolization Beads (DEBs) have been developed primarily for the locoregional treatment of malignancies in the liver by means of minimally invasive delivery through Trans-arterial Chemoembolisation (TACE) (Nicolini et al., 2011). There are now several commercially-available devices on the market that are all generally composed of hydrogel microspheres of calibrated sizes that are capable of interacting with certain drugs by an ion-exchange process (Facciorusso, 2018; de Baere et al., 2016). For example, DC Bead™ are composed of a polyvinyl alcohol (PVA) hydrogel modified to contain negatively charged sulfonate groups, enabling ionic interaction with positively charged drugs which is reversible in ion-rich environments such as blood (Lewis, 2009). These devices are supplied to the hospital pharmacy where they are loaded with the appropriate chemotherapeutic drug and then supplied to the physician for administration using X-ray guided navigation through the blood vessels into the liver in order to target the site of the tumour. The choice of drug is dependent upon the type of liver tumour being treated and the physician's preference. For the treatment of hepatocellular carcinoma (HCC, primary liver cancer) (Lammer et al., 2010) or certain tumours that have spread to the liver such as breast cancer metastases (Martin et al., 2012), the most common agent selected is doxorubicin hydrochloride at a dose of 25 or 37.5 mg/mL of hydrated beads, but in some instances structurally similar anthracycline drugs such as epirubicin (Nicolini et al., 2010) or idarubicin (Boulin et al., 2014) have been used as alternatives. On the other hand, metastatic colorectal cancer (mCRC) to the liver has been treated with DEBs loaded with irinotecan hydrochloride using a slightly modified administration technique (Martin et al., 2009, 2011; Taylor et al., 2007). Most recently there has been much interest in the delivery of other more targeted therapeutic agents from DEBs, in particular the multi-tyrosine kinase inhibitors (MTKi) which have inhibitory effects on tumour microvasculature (Fuchs et al., 2014; Hagan et al., 2017; Lahti et al., 2015). Indeed, the first HCC patients have recently been

* Corresponding author at: School of Pharmacy and Biomolecular Sciences, University of Brighton, Moulsecoomb, Brighton BN2 4GJ, UK.
E-mail addresses: alice.hagan@outlook.com (A. Hagan), andrew.lewis@btgplc.com (A.L. Lewis).
[1] Authors contributed equally.

https://doi.org/10.1016/j.ejps.2019.05.021
Received 19 October 2018; Received in revised form 3 May 2019; Accepted 27 May 2019
Available online 29 May 2019

treated in a clinical trial where the MTKi vandetanib has been pre-loaded onto a DEB, in this case a newer device platform which is also radiopaque in nature and therefore can be visualized intra and post-procedurally using X-ray based imaging methods (Ashrafi et al., 2017; Duran et al., 2016; ClinicalTrials.gov, 2017).

As interest in DEB-mediated local delivery of different chemotherapeutic drugs grows, there is a need to be able to screen these agents using *in vitro* methodologies that provide some level of prediction as to how the drug may be released *in vivo*. There have been many different types of elution test described for the evaluation of DEBs, including simple USP Type II apparatus studies which are suited for Quality Control tests to ensure uniformity between batches, but are uninformative on how the products will release drug once placed within a blood vessel (Gonzalez et al., 2008). USP Type IV and T-cell Apparatus have been shown to be more predictive of the *in vivo* situation, as they allow for elements of drug diffusion and convection (Gonzalez et al., 2008; Amyot et al., 2002; Fuchs et al., 2015; Jordan et al., 2010). As drug elutes from the beads and travels through the embolised vessel walls into tissue, the drug's physicochemical properties will dictate how it diffuses and interacts with cells or is eventually carried away as it enters more distant vessels in which blood flow is maintained. Elements of drug metabolism however, cannot be easily accommodated in these models. More recently, we have described an open-loop flow through system which under the right conditions can be representative of the long-term release that has been observed for doxorubicin in explanted tissues (Swaine et al., 2016). None of these methods however, are particularly applicable to the initial 24 h post-delivery of the beads, where the peak plasma concentrations (C_{max}) can be a predictor of the levels of systemic toxicity that might be experienced by the patient (Song & Kim, 2017; Lencioni, 2012).

The reason for this lack of correlation is because established *in vitro* tests usually begin with a "pre-occluded system" in which the beads have already been placed into a situation that represents a post-administration occlusive mass (Caine et al., 2017a). In order to properly evaluate how a DEB will respond to delivery *in vivo*, the administration phase must also be mimicked as per the schematic in Fig. 1. The beads must be mixed with contrast agent before delivery, which, depending on the ionic composition of the contrast agent, can induce in itself a small degree of drug elution from the surface layers of the beads. The bead/contrast suspension is then slowly delivered in small "puffs" at a rate of around 1 mL of suspension per minute in order that the beads are carried by the blood into the arterial high flow areas (normally the tumour when it is hypervascular in nature) and distribute into the distal arterioles without premature proximal blockage (phase 1, the initial 15–30 min during bead delivery). If the drug-bead interaction is weak, caused for example by steric hindrance and/or charge delocalisation at the drug binding site (Biondi et al., 2013), there may be a burst of drug release during this phase as the beads are surrounded by ion-rich blood which is an effective medium for the sequestration of drug (Jordan et al., 2010; Taylor et al., 2007). Beads will fill vessels distally and compact until they form a cast within the vessel architecture and flow between and around the beads is slowed to near stasis (phase 2, which starts to occur whilst the beads are still being delivered but would represent the next 15–30 min as the beads redistribute and compact into the vessels). Finally, the stagnated blood between the beads will eventually clot to form an occlusive mass, and ions from the surrounding tissues will diffuse into the mass and exchange for the drug bound to the bead reservoirs, leaving the drug to diffuse into the surrounding tissues by mass transfer (phase 3, which starts to occur once the beads have formed an occlusive mass and can continue for days to weeks depending upon the drug and dose delivered).

In this study, we report for the first time on a drug elution test method that mimics the drug release during the DEB administration procedure (phases 1 and 2 in Fig. 1) and provides a vehicle for a semi-quantitative prediction of drug plasma exposure over the first 24 h post DEB delivery. The ability to predict this early phase of drug release is of fundamental importance in the evaluation of these products, as this dictates the peak plasma levels and hence systemic exposure to the drug and likelihood of drug-related toxicities. This was achieved by comparing the drug elution profiles generated using both a custom-built Vascular Flow System (VFS) and the previously reported open-loop method, with the pharmacokinetic data obtained from the swine hepatic artery embolization model. Doxorubicin release from standard DEB (DC Bead™) was compared to that from a radiopaque DEB (DC Bead LUMI™), followed by an evaluation of elution of three different drugs loaded onto the radiopaque drug-eluting bead: doxorubicin (LUMIDOX), irinotecan (LUMIRI) or vandetanib (LUMIVAN). These drugs were chosen as they have all been used in the clinic for the treatment of hepatic malignancies.

2. Methods

2.1. Materials

DC Bead™ and DC Bead LUMI™ (both 70–150 µm) were provided by Biocompatibles UK Ltd. (Farnham, UK). Doxorubicin HCl (Zheijan Hisun Pharmaceutical Co., China), irinotecan HCl (ScinoPharm, Taiwan) and vandetanib (> 99% purity, Sanofi Genzyme, UK) were supplied as powders and dissolved in ultrapure water to the desired concentration to provide drug loading solutions. Vandetanib solution was acidified to pH 4.7 with hydrochloric acid to aid drug solubility. Non-ionic contrast agent composed of 755 mg/mL iohexol

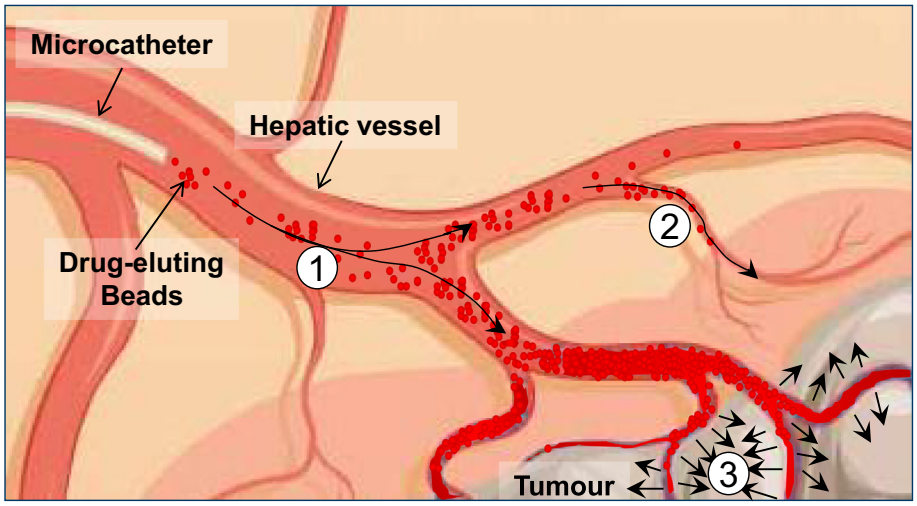

Fig. 1. Schematic of the phases of DEB delivery. Phase 1: DEB suspension is injected *via* the hepatic artery and exposed to free flowing, ion-rich blood. Phase 2: DEB begin to embolise distal vessels inducing near stasis of blood flow. Phase 3: DEB establish clots in tumour vessels and drug is released into tissue *via* diffusion.
Adapted from (Caine, 2017).

(Omnipaque™ 350) was purchased from GE healthcare (UK). Phosphate buffered saline (PBS), (pH 7.0, 137 mM NaCl) was used as the *in vitro* elution medium and was purchased from Source Bioscience (Nottingham, UK).

2.2. Drug-loading of beads

Beads were loaded with doxorubicin, irinotecan and vandetanib at 37.5 mg, 50 mg and 100 mg per mL of hydrated beads, respectively. Specifically, this involved removal of the saline packing solution with a pipette to leave an approximate volume of 2 mL of bead slurry with minimal remaining liquid. The appropriate volume/concentration of drug was added to the vial containing the slurry to achieve the desired loading and left for a minimum of 1 h for doxorubicin and irinotecan and 2 h for vandetanib, with occasional agitation.

2.3. Drug-loaded bead characterization and contrast agent compatibility

Optical microscopy was used to investigate morphology of radiopaque beads post drug loading. DEBs were placed in Petri dishes in a monolayer and an Olympus BX50 microscope with attached Colorview III camera was used to capture optical micrographs of each bead sample. Calibrated sizing software (Stream, Olympus, UK) was used to measure the diameter of 200 beads per sample.

1 mL of each DEB was suspended in 10 mL of neat contrast agent (Omnipaque 350) by transfer between two syringes *via* a 3-way connector. To assess drug release into the contrast agent, the suspensions were stored at room temperature and aliquots of contrast agent were analysed for drug content over a 24 h period by High Performance Liquid Chromatography (HPLC) (see Supplementary Information for method details).

2.4. Early phase elution model: the Vascular Flow System

The Vascular Flow System (VFS) used to study drug elution during the administration phase was based on the apparatus previously described for use in the investigation of the flow dynamics of Y90 microspheres (Caine et al., 2017b). The system is comprised of a silicon cast (Elastrat Sarl, Geneva, Switzerland) with circular channel cross-sections, a 4-mm inlet, and six 0.9-mm outlets (Fig. 2A). In this instance, the VFS, positioned flat on the bench, was circulated with PBS pre-warmed to 37 °C using a peristaltic pump to induce pulsatile flow of 120 mL/min and the circuit modified as shown in Fig. 2(A). A microcatheter (Progreat® 2.4 F, Terumo, Belgium) was steered into a fixed location beyond the first bifurcation point (red arrow, Fig. 2(A)), in order that two of the six outlet filters became the target embolization sites, which were accordingly blocked with a 27 μm mesh (Sefar AG, Switzerland). The remainder of the outlets, not being exposed to the DEBs, were recirculated back into the PBS reservoir. DEB/contrast agent suspensions as prepared in Section 2.3 were then slowly administered into the VFS using a syringe pump set at a continuous rate of 1 mL/min where upon the beads would exit the microcatheter and collect in the outlet filter, producing an occlusive mass and reducing the eluent flow. The eluent was collected from these outlets, starting from the initiation of the DEB delivery and every minute for the first 10 min then every 5 min until a 30 minute test period was complete. Drug concentrations in the eluent at each collection time point were determined using UV spectroscopy (doxorubicin, 483 nm; irinotecan 369 nm) or HPLC (method for vandetanib analysis in supplementary information) and an elution curve was constructed from the data.

2.5. Mid phase elution model: open loop flow through system

Drug release from radiopaque beads was also profiled in a slow rate, flow through cell open loop system (Fig. 2(B)) as described previously (Swaine et al., 2016). Drug loaded beads (1 mL settled volume) were sandwiched between two filter membranes in an elution cell, submerged in a water bath maintained at 37 °C and protected from light. PBS was pumped through the system at a flow rate of 0.1 mL/min, in order to mimic slow residual blood flow after embolization. Detection of drug concentration in the eluent over time was performed by automated UV spectroscopy of eluent passing through a flow through cuvette (doxorubicin, 483 nm; irinotecan, 369 nm; vandetanib, 330 nm). Drug concentration was calculated from absorbance data using standards of known concentration for each drug to enable construction of elution curves.

2.6. Swine hepatic artery embolisation procedure

In order to compare the *in vitro* elution profiles with relevant *in vivo* data, pharmacokinetic data was obtained from a pre-clinical study of transarterial chemoembolization (TACE) using drug-eluting beads in healthy swine. The embolisation procedure was carried out at MPI Research (Mattawan, Michigan, USA) using experimentally naïve male domestic Yorkshire crossbred swine (farm pigs, weights 53.5–66.5 kg at randomization), as previously described (Denys et al., 2017). The research centre is AAALAC accredited and the study conformed to USDA Animal Welfare Act (9 CFR parts 1, 2 and 3) and to the 'Guide for the Care and Use of Laboratory Animals', Institute of Laboratory Animal Resources, National Academy Press, Washington, D.C, 2011.

In brief, each DEB, loaded as described in Section 2.1, was suspended in Omnipaque 350 contrast agent (an iodinated compound in aqueous solution that is injected into the blood vessels to render the vessels visible under X-ray imaging). In accordance with their respective instructions for use, DC Bead were suspended in a 50:50 contrast agent: saline mixture and DC Bead LUMI were suspended in neat contrast agent. In both cases the ratio of beads to contrast or diluted contrast was 1:10. Uniform suspensions were achieved by mixing between two syringes *via* 3-way stopcock. The bead suspension was aliquoted into a 3 mL syringe for delivery through the microcatheter to allow for better control and re-suspended regularly to prevent sedimentation. Access and selection of the main hepatic artery was achieved using a 2.7 Fr microcatheter (Progreat®, Terumo Japan). An arterial branch that fed around 50% of the liver volume was identified and an angiogram of the liver lobe(s) taken. With the catheter in position at the target location, the selected DEB was administered slowly under continuous fluoroscopy, evaluating changes in vascular flow rate and appearance of reflux or non-target embolization of the beads (inferred from visible contrast flow). The maximum volume was administered for all animals (target volume 1 mL of sedimented beads). Dosing occurred in the left lateral lobe or left median lobe for all animals. After all images were obtained, all guides, catheters, and the sheath were removed and the femoral artery ligated; the muscle and subcutaneous tissues were closed with absorbable sutures and the skin was closed with skin glue.

Blood samples were collected from all animals *via* the jugular or ear vein for determination of the plasma concentrations of doxorubicin, irinotecan, or vandetanib. Samples were collected pre-dose and at selected intervals following administration, up to 14 days. Plasma was analysed for the concentration of doxorubicin, irinotecan or vandetanib using validated LC-MS-MS methods specific to each drug (see supplementary information). Individual doxorubicin, irinotecan, and vandetanib plasma concentration-time profiles from treated animals were analysed using model independent methods in Phoenix® WinNonLin® software (Certara, USA). For each animal, the following plasma pharmacokinetic parameters were determined: maximum observed plasma concentration (C_{max}), time of maximum observed plasma concentration (T_{max}), and area under the plasma concentration-time curve (AUC). The AUC from time 0 to 336 h ($AUC_{0–336h}$), the AUC from time 0 to the time of the final quantifiable sample (AUC_{Tlast}), and the AUC from time 0 to infinity (AUC_{INF}) were calculated by the linear trapezoidal method for all animals with at least three consecutive quantifiable concentrations.

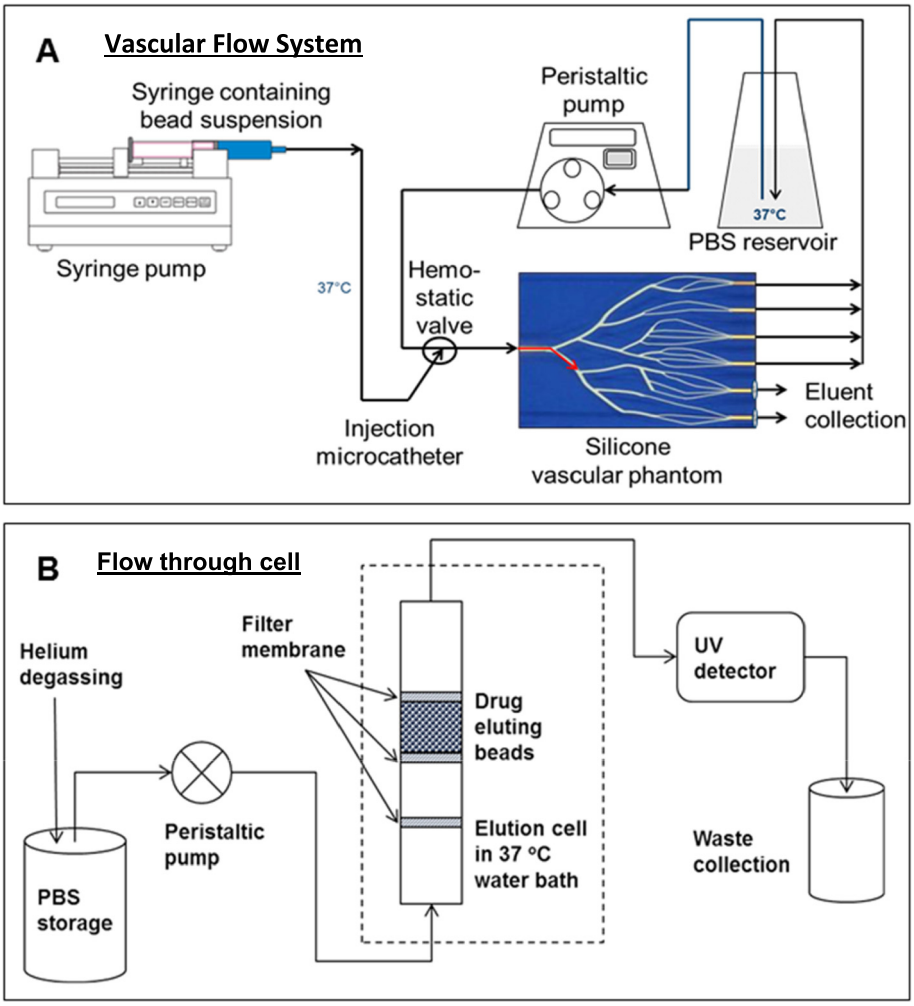

Fig. 2. Schematics of *in vitro* elution models (Adapted from Caine et al. (2017b)). A) In the vascular flow system, bead suspensions are delivered at a constant rate *via* a syringe pump into a silicone vascular phantom. Mesh inserts at selected channel ends obstruct the beads forming an occlusion through which PBS is collected and analysed for drug content. B) In the flow through cell, beads are sandwiched between filter membranes (Adapted from Swaine et al. (2016)). PBS is pumped at a rate of 0.1 mL/min through the column to be analysed for drug content *via* UV spectroscopy. (For interpretation of the references to colour in this figure, the reader is referred to the web version of this article.)

Table 1
Pharmacokinetic parameters obtained from the pre-clinical embolisation studies in healthy swine liver.

DEB	Drug dose (mg)	C_{max} (ng/mL)	C_{max}/Dose (ng/mL/mg)	T_{max} (hr)	AUC_{Tlast} (hr∗ng/mL)	AUC_{Tlast}/Dose (hr∗ng/mL/mg)	$T_{½}$ (hr)	V_d (L/kg)
LUMIDOX *n* = 3	37.5	74.6 ± 27.7	1.99 ± 0.74	0.067 (0.067–0.15)	185 ± 24.6	4.93 ± 0.657	N/A[a]	N/A[a]
LUMIRI n = 3	50	474 ± 138	9.47 ± 2.77	1.067 (0.4–2.2)	2860 ± 278	57.3 ± 5.57	3.67 ± 0.74	1.47 ± 0.42
LUMIVAN *n* = 8	100	23.8 ± 9.13	0.238 ± 0.09	2 (0.333–4)	535 ± 150	5.35 ± 1.5	22.8 ± 4.15	97.4 ± 26.4

[a] Parameter could not be calculated due to insufficient plasma-concentration time data.

Half-life values ($T_{1/2}$) were reported for each plasma concentration-time profiles that had sufficient plasma concentrations in the terminal elimination phase (at least three samples not including T_{max}) and an adjusted R^2 of ≥0.9.

2.7. *In vitro in vivo correlation (IVIVC)*

Two approaches for IVIVC were used depending on the elution model being evaluated. For the early phase VFS model, the effect of drug elimination was considered less important due to the short duration (30 min) of the experiment. Therefore, a simple point to point comparison was made between plasma AUC calculated with the trapezoidal method, plotted against % cumulative release *in vitro*, in order to assess correlation.

For the later phase flow through elution data, a convolution method was used to convert *in vitro* dissolution profile to a predicted plasma profile using the method described by Qureshi (Qureshi, 2010). The amount of drug released between time points (amt (mg)) was calculated and a first order elimination model was applied to determine drug elimination over time. The sum of the drug amount remaining (in mg) for each time point was then converted to a predicted plasma concentration (C) in ng/mL (Eq. (1)).

$$C = \frac{amt \times 1000}{V_d \times body\ weight} \quad (1)$$

where V_d is the volume of distribution of the drug expressed in L/kg. Bioavailability was considered to be 100% due to intra-arterial administration, therefore was not accounted for in the equation. $T_{1/2}$ and V_d for vandetanib and irinotecan in swine were obtained from calculated values reported in the pre-clinical study reports for LUMIVAN and

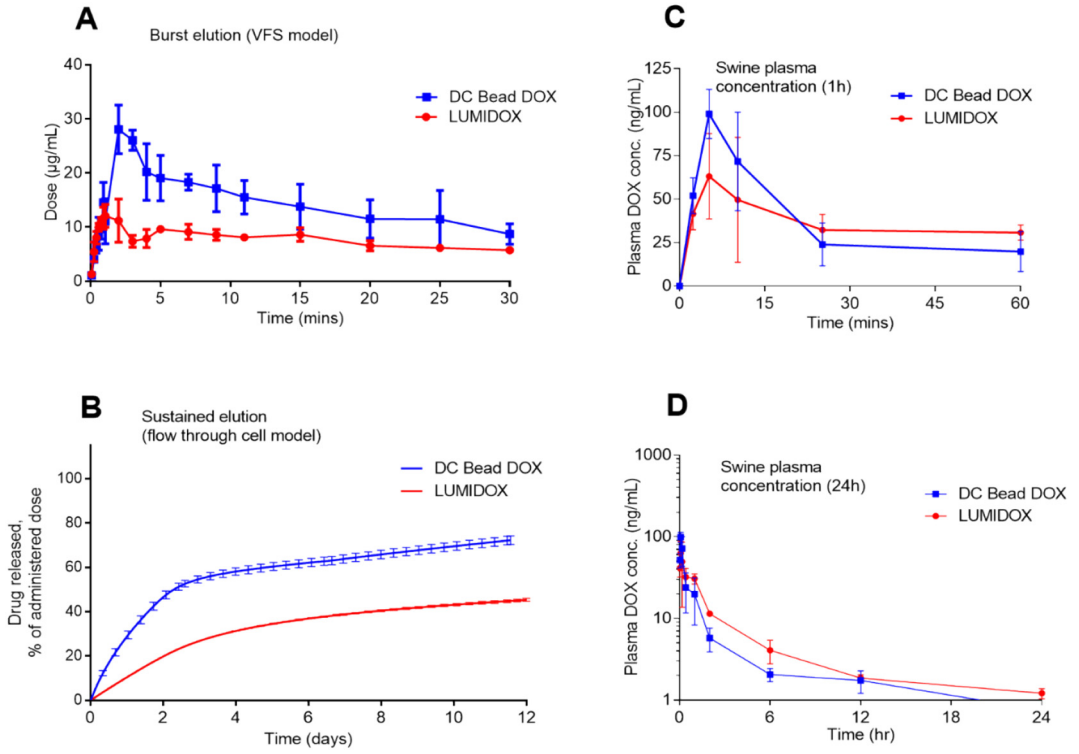

Fig. 3. Comparison of doxorubicin elution from non-radiopaque DC Bead and radiopaque DC Bead LUMI (37.5 mg/ml). A) Dox elution in the VFS model, B) percentage dox release in the slow flow through model, C) plasma concentrations of doxorubicin after DEB-TACE procedures in swine for the first hour and D) first 24 h.

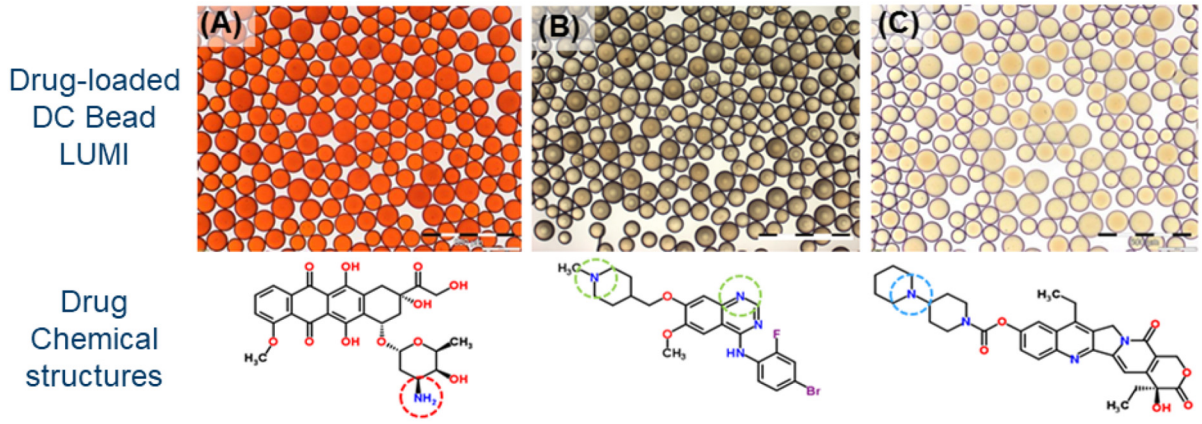

Drug Properties	Doxorubicin	Vandetanib	Irinotecan
Molecular Formula	C27H29NO11	C22H24BrFN4O2	C33H38N4O6
Molecular weight	543.525 g/mol	475.362 g/mol	586.689 g/mol
LogP (log Kow)	1.27	5.0	3.2
Water solubility (neutral form)	2600 mg/L at 25°C	8 mg/L at 25°C	107 mg/L at 25°C
Bead loading dose	37.5 mg/mL	100 mg/mL	50 mg/mL

Fig. 4. Optical micrographs of A) LUMIDOX, B) LUMIVAN and C) LUMIRI, scale bars 500 µm. Chemical structures for each drug are shown with protonated amine groups (site of drug – bead ionic interaction) circled. Physicochemical properties for each drug are listed in the table beneath.
(Source: NIH PubChem open chemistry database)

LUMIRI (See Table 1). These values were not able to be calculated for LUMIDOX, therefore $T_{1/2}$ and V_d for doxorubicin in swine were obtained from the literature, 2.6 h and 4.86 L/kg respectively (Dubbelboer et al., 2014). Average pig body weights in kg were obtained from the pre-clinical study reports. AUC of the predicted and actual plasma profiles between $t = 0$ and the last shared time point for which $C > 0$ were calculated using the trapezoidal method and correlated.

3. Results

3.1. Comparison of non-radiopaque and radiopaque microspheres

The elution and plasma profiles of the non-radiopaque DC Bead were firstly compared with the radiopaque DC Bead LUMI, to understand the influence of bead chemistry on elution rates in the different models with doxorubicin as a representative drug (Fig. 3). The *in vitro* models demonstrated that doxorubicin is released from DC Bead LUMI at a slower rate than from DC Bead, as evidenced by a smaller elution 'burst' and C_{max} in VFS model, a pattern which was well reflected in the early swine pharmacokinetic profile (Fig. 3A & C). The slow flow through cell model also showed a difference between the two bead types, with the radiopaque beads releasing a lower proportion of the doxorubicin dose compared with non-radiopaque beads: 40% of the dose was eluted after 12 days compared with 70% for DC Bead (Fig. 3B). However, the level of doxorubicin in the plasma declined at a similar rate for both bead types, reaching low levels (< 1 ng/mL) by 24 h and becoming undetectable by 72 h after administration (Fig. 3D).

3.2. Radiopaque drug-loaded bead characterization and leaching in contrast agent

Focusing on the radiopaque bead platform, the characteristics of DEBs loaded with the three different drugs were then examined. Loading of the radiopaque beads with the various drugs under study led in each case to a DEB formulation consisting of perfectly spherical and smooth beads with a precisely identified drug dose and within the specified 70–150 μm size range (averages between 90 and 100 μm) as shown in Fig. 4.

The amount of drug released from radiopaque DEBs during contrast agent storage over a 24 h period was shown to vary depending on drug type. The amount of vandetanib released from LUMIVAN into the contrast medium 15 min after mixing was 3.3 mg, which increased to just 3.5 mg in total after 24 h storage at room temperature representing 3.5% of the loaded dose. On the other hand, irinotecan was quickly leached from LUMIRI upon mixing with contrast agent, and the amount released continued to increase with extended storage, from 1.9% (immediately after mixing) to 10.8% (4 h). LUMIDOX was stable in contrast agent and eluted only 0.2% of the loaded dose in up to 4 h of storage. There was no further leaching of irinotecan or doxorubicin after 4 h, suggesting equilibrium concentrations were achieved for these drugs in the given volume of contrast agent.

3.3. In vivo pharmacokinetics of radiopaque DEB (swine study)

The pharmacokinetic profiles for the three drugs are seen to be different in each case when comparing the curve shapes in Fig. 5(A), which shows the respective plasma concentrations for each drug over the first 24 h following DEB administration. The C_{max} (see also Table 1) for LUMIRI is much higher than for LUMIDOX and LUMIVAN. LUMIDOX reaches C_{max} within minutes and declines rapidly, whereas LUMIRI takes between 1 and 2 h and declines over the next 24 h. LUMIVAN shows a relatively low C_{max} at about 1 h and persists in the plasma with a slow decline over several days. Fig. 5(B) provides an alternative 24 h plot whereby double Y axes are used to allow the LUMIRI to be scaled to the same order of magnitude as the other DEBs, and Fig. 5(C) shows the same data over a 120 h period to demonstrate the long period over which vandetanib can be detected in the plasma post administration.

Plotting the $\log_{10}$ of plasma concentrations (Cp) *vs* time resulted in different slopes for the different drugs (Fig. 5(D)). Vandetanib and irinotecan showed a linear relationship between log Cp and time, indicating that the pharmacokinetics of these drugs are best fit by a one-compartment model. On the other hand, doxorubicin pharmacokinetics appeared to be more multi-phasic, which suggests a multi-compartment model may be applicable, as has been previously suggested (Gustafson et al., 2002; Reich et al., 1979).

3.4. Early phase in vitro drug release (VFS model)

The drug release profile obtained using the VFS elution model representing the first 30 min of bead administration is shown in Fig. 6 represented as raw concentration time data (A) and cumulative release as percentage of the total dose (B). The elution rate peaks within the first 5 min, demonstrating a 'burst' effect that is clearly more pronounced with irinotecan than with vandetanib or doxorubicin. The accumulation of beads in the channel ends led to a dramatic decrease in eluent flow rate passing through the occlusive bead mass, which corresponded with the drop in elution rate. The flow rate profile was similar for each DEB tested. The amount of drug released over 30 min corresponded to approximately 9% of the total dose for irinotecan, 2.6% for doxorubicin and 2.1% for vandetanib.

Fig. 6(C) shows the correlation of the VFS elution data with the first 30 min of the *in vivo* plasma pharmacokinetic profiles. The AUC of doxorubicin and irinotecan plasma profiles were calculated using the trapezoidal method, and plotted against cumulative % release from the VFS elution data at corresponding time points (2, 5, 11, 25 min from start of bead administration). Doxorubicin showed a more linear correlation than irinotecan, but in both cases the data appeared better fitted by an exponential curve, indicating that drug was released faster *in vitro* than *in vivo*. T_{max} for doxorubicin were in a similar timeframe *in vitro* and *in vivo* ($t = 0.9$ min *vs* $t = 4$ min respectively). The difference was greater for irinotecan, with the VFS showing T_{max} to be 2 min, whereas maximal plasma concentrations were seen at approximately 1 h in the swine model. The frequency of blood draws in the vandetanib bead swine pre-clinical study was not sufficient to allow a point-to-point correlation with VFS data. However, T_{max} were compared and also found to differ significantly, with the VFS model showing T_{max} at 3 min compared with 2 h *in vivo*. The dose adjusted C_{max} values were not drastically different between *in vivo* and *in vitro*, indicating that similar proportions of the drug dose contained within the beads were released in the early phase set up, albeit at an accelerated time course. The compared C_{max} and T_{max} for each drug are summarised in Fig. 6(D).

3.5. Later phase in vitro drug release (open loop flow through model)

Comparison of the later phase release (post formation of an occlusive mass of beads) of the various DEBs as modelled using the open-loop flow through model is shown in Fig. 7(A) as dose with time (expansion inset 7(B)), and Fig. 7(C) as cumulative percentage dose released. Using this method, irinotecan is still seen to release relatively rapidly compared to the other drugs with complete release achieved in around 2 days. Doxorubicin displays a sustained and slow elution, with around 45% of the dose eluted within 16 days and continuing at a slow rate. Vandetanib displays an intermediate release pattern, with a linear zero order release phase over the first 5 days that plateaus after 90% is eluted.

Comparing the raw concentration-time data for the flow through model with the *in vivo* PK data, we see that the T_{max} are fairly similar to their *in vivo* counterparts for vandetanib and irinotecan (3 h *vs* 1 h, 2.2 h *vs* 2 h respectively), but the duration of drug release in the model persists longer than the presence of drug in plasma.

In order to achieve optimal IVIVC, a linear correlation would be

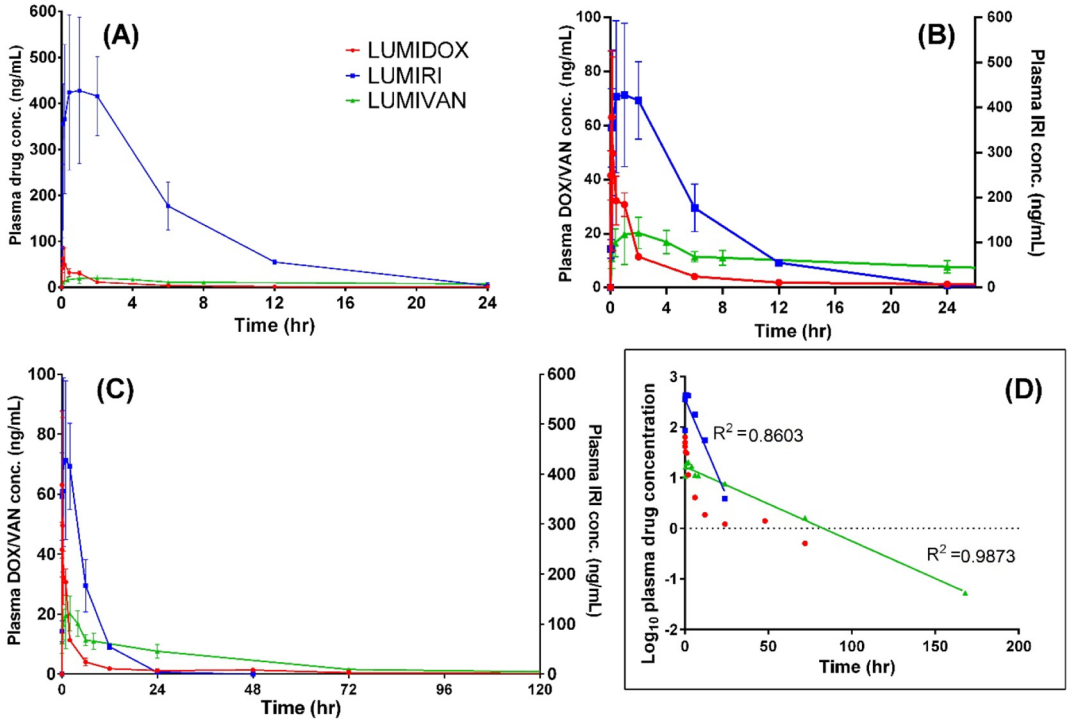

Fig. 5. Plasma drug concentrations (Cp) over time following administration of 1 mL LUMIDOX 37.5 mg/mL [red circles] LUMIRI 50 mg/mL [blue squares] or LUMIVAN 100 mg/mL [green triangles] in healthy swine liver. A) Cp *vs* time, 24 h plot. B) Cp *vs* time with DOX and VAN plotted on left axis, IRI plotted on right axis. C) Cp *vs* time as in (B) over 120 h period. D) Log 10 Cp *vs* time showing linear correlation for LUMIRI ($p = 0.0003$) and LUMIVAN ($p < 0.0001$). Data are mean of $n \geq 3$ animals ± SD.

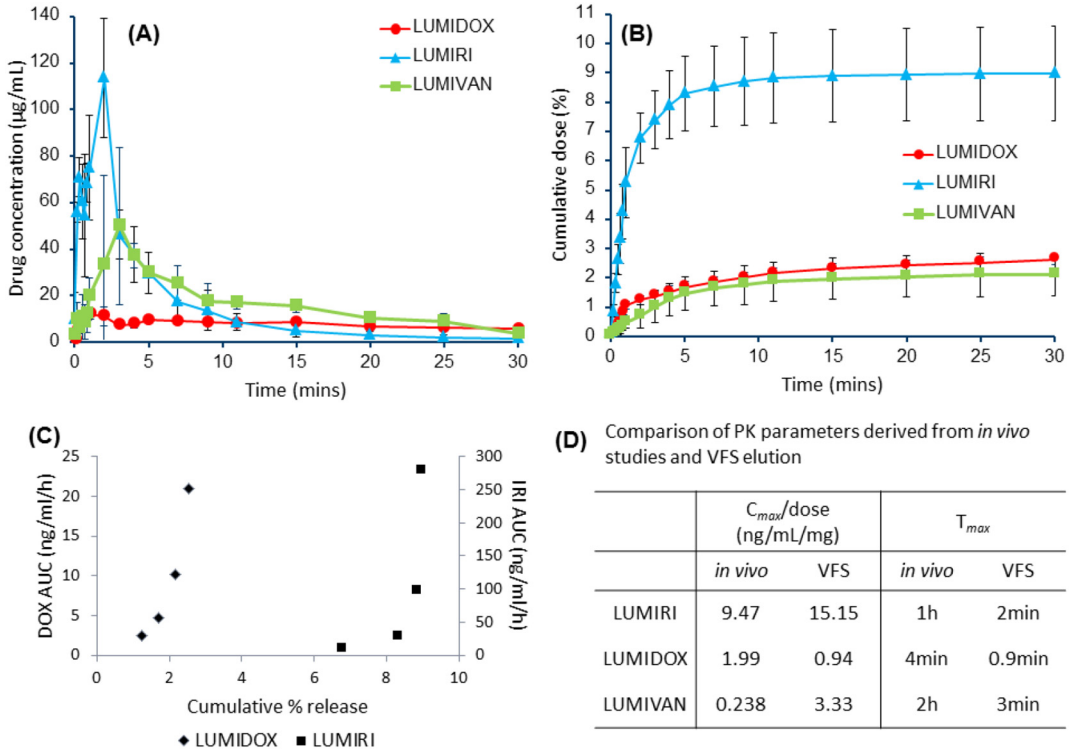

(D) Comparison of PK parameters derived from *in vivo* studies and VFS elution

	C_{max}/dose (ng/mL/mg)		T_{max}	
	in vivo	VFS	*in vivo*	VFS
LUMIRI	9.47	15.15	1h	2min
LUMIDOX	1.99	0.94	4min	0.9min
LUMIVAN	0.238	3.33	2h	3min

Fig. 6. Drug release data obtained following injection of 0.15 mL DEB aliquots using the VFS model, and IVIVC. A) Drug concentration *vs* time plot demonstrates early burst release in the first 5 min. B) Drug release in the VFS as a cumulative percentage of total available dose. C) AUC data from *in vivo* studies (left axis LUMIDOX, right axis LUMIRI) is plotted against cumulative % release in VFS for the first 30 min following DEB delivery to assess IVIVC. LUMIVAN was not plotted due to lack of comparable time points. D) Comparison of PK parameters derived from *in vivo* swine studies and VFS model show similarities in dose adjusted C_{max}.

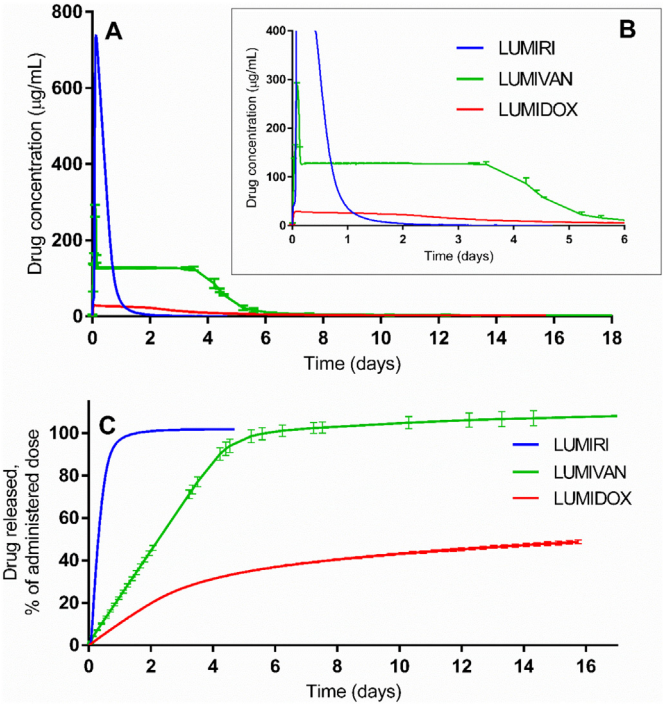

Fig. 7. Drug release profiles obtained using the flow through cell model. A) Raw concentration time data, B) (inset) expanded view of the first 6 days. C) Data plotted as cumulative release as percentage of total dose.

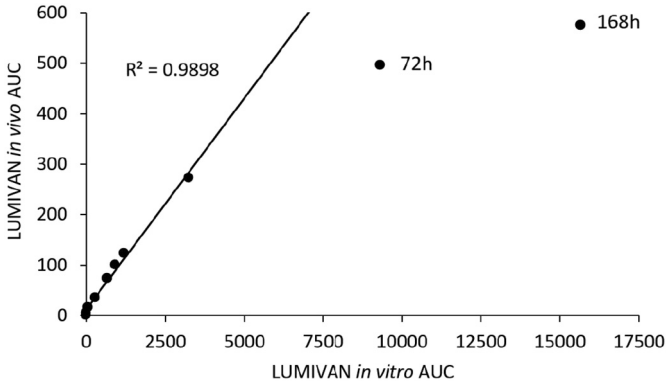

Fig. 8. Assessment of IVIVC between *in vitro* and *in vivo* AUC from raw LUMIVAN flow through elution data. Linear correlation was achieved for the first 24 h ($p < 0.0001$). Later time points (72 h and 168 h) were excluded from the linear regression analysis.

expected between compared parameters over the complete time course. Interestingly, despite differing by an order of magnitude, when *in vitro* and *in vivo* AUC were plotted against each other, a linear correlation was achieved for LUMIVAN for the first 24 h, but not for LUMIRI or LUMIDOX (Fig. 8). AUC calculated from the raw concentration time data from the flow through model correlated better than the convoluted data in this case, but both fits had an $r^2 > 0.9$. The steep slopes of the compared AUCs for doxorubicin and irinotecan in the first hour is indicative of the drug being observed in the plasma *in vivo* much faster than it was observed in the *in vitro* test (data not shown).

The raw *in vitro* data from the slow flow through model were convoluted using a first order elimination model as described in Eq. (1) (Fig. 9). The convoluted flow through data for LUMIVAN and LUMIRI showed similarity in curve shape to the plasma profiles, predicting a similar elimination time course for the drugs from the plasma. The convolution was not extended past 48 h due to the infrequency of comparable data points beyond this time: the average plasma T_{last} for LUMIRI, LUMIDOX and LUMIVAN were 12 h, 48 h and 72 h respectively. The predicted maximum plasma concentrations as well as AUC for all DEBs were between 5.2 and 66.3-fold lower than the actual values, however at later stages (24–48 h) the predicted and actual concentrations begin to converge. The *in vitro* T_{max} in all cases occurred several hours later compared with *in vivo*. For doxorubicin, the convoluted elution profile did not correlate well in terms of curve shape with the actual plasma profile, predicting a much lower C_{max} and slower elimination of the drug. However, from 12 h onwards, the predicted and actual doxorubicin concentrations are within 1–2 ng/mL of each other, which may explain why the compared AUCs differed less than the C_{max} values.

4. Discussion

4.1. Effect of drug chemistry on release from DEB

Drug release from the DEBs used in this study is based on ion exchange (Lewis, 2009). Upon contact with biological fluids, small cations exchange with the positively charged drug molecules in the microsphere matrix. The rate controlling mechanisms for different drugs, for example doxorubicin and irinotecan, have been found to vary based on differing molecular interactions between drug and bead (Biondi et al., 2013), which explains differences in release rates observed both *in vitro* and *in vivo*. Doxorubicin binds *via* a primary amine group, which is expected to interact more strongly with the beads than irinotecan's tertiary amine, and also exhibits pi-pi stacking which could be a cause of drug aggregation within the bead leading to slow elution (Ahnfelt et al., 2016). Indeed, a high propensity to form aggregates has been correlated with slower release rates of amphiphilic substances from DEBs (Ahnfelt et al., 2018). Vandetanib possesses two potential ionic binding sites dependent on the pH and subsequent protonation state of the molecule (see Fig. 4): at pH 7, only the tertiary amine is protonated, whilst at loading pH (4.6–4.8) 30–40% of molecules are expected to carry an additional positive charge in the pyrimidine group. We have previously described how this property affects the vandetanib loading capacity into DEB due to occupation of multiple binding sites per molecule, however it does not significantly affect the drug release rate of beads loaded at different pH due to partial charge neutralisation in the pH 7 PBS elution medium (Hagan et al., 2017). It does however, explain why vandetanib is released more quickly from the open-loop flow-through method than expected based on solubility of the free-base alone, as the protonated form is released from the bead and remains partially protonated and hence more soluble within the PBS. In the models employed in this study, vandetanib was released from DEBs more slowly than irinotecan, but faster than doxorubicin, suggesting it forms weaker drug – bead interactions than the latter and/or lacks the drug-drug interactions that exist for doxorubicin. This resulted in the complete release of vandetanib from DEB in the flow through model after ~10 days, whereas complete doxorubicin release was not achieved after 2 weeks. This is in line with a previous *in vivo* study, where < 50% of the doxorubicin dose contained with DC Beads was found to be released 28 days after implantation in swine liver (Namur et al., 2010).

The chemistry of the bead matrix also plays a role in drug release rates, as has been previously demonstrated in comparison of DC Bead and the radiopaque DC Bead LUMI (Hagan et al., 2017; Ashrafi et al., 2017). Despite the drug binding mechanism being theoretically unaltered, the matrix is rendered more hydrophobic and dense by the addition of the radiopaque moiety, reducing the size of the water-filled channels in the hydrogel matrix and impeding transport of drug molecules within the beads. This led to a slower drug release *in vitro* and a lower plasma C_{max} in the swine pharmacokinetic study, which suggests a reduced systemic exposure to the drug. However, it has not yet been determined whether this difference is significant enough to translate into clinically meaningful differences in systemic toxicity.

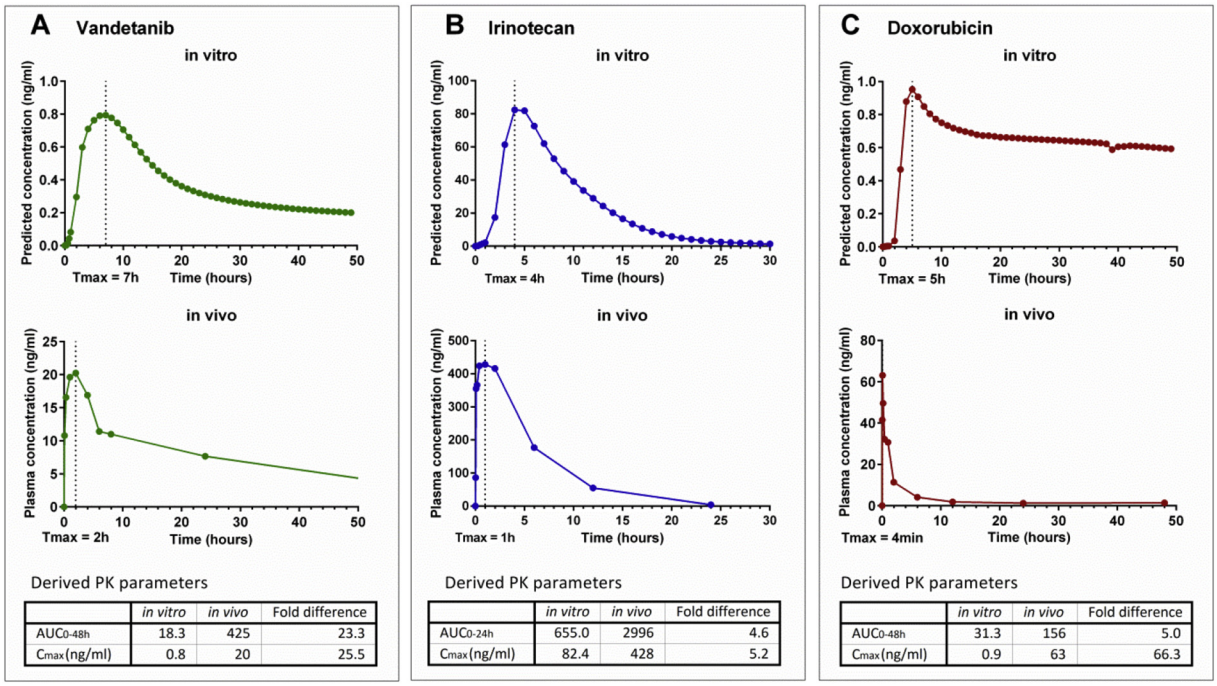

	in vitro	*in vivo*	Fold difference
$AUC_{0\text{-}48h}$	18.3	425	23.3
C_{max} (ng/ml)	0.8	20	25.5

	in vitro	*in vivo*	Fold difference
$AUC_{0\text{-}24h}$	655.0	2996	4.6
C_{max} (ng/ml)	82.4	428	5.2

	in vitro	*in vivo*	Fold difference
$AUC_{0\text{-}48h}$	31.3	156	5.0
C_{max} (ng/ml)	0.9	63	66.3

Fig. 9. Convoluted flow through cell elution data (top row) compared with *in vivo* plasma concentration (bottom row) for A) LUMIVAN, B) LUMIRI and C) LUMIDOX and comparison of *in vitro* and *in vivo* PK parameters (tables inset).

4.2. Evaluation of the in vitro elution models

4.2.1. VFS model

The VFS model allows the reproduction of many phenomena experienced during administration of DEB in the clinic: suspension in contrast agent, gradual (rather than instantaneous) DEB delivery, exposure to high rate pulsatile flow of elution medium, and eventual packing of beads in a confined channel. The presence of these features is a vast improvement in representativeness of the *in vivo* situation, in comparison to the basic USP type set-ups. This may have been key to having achieved correlation of the elution data with the first 30 min of *in vivo* plasma concentration data in the case of doxorubicin release from both DEB platforms. For LUMIRI and LUMIVAN the model predicted an earlier T_{max} than the *in vivo* value. However, the dose adjusted C_{max} were in a similar range to the *in vivo* values for all three drugs, suggesting that the model may be useful in predicting the extent of burst release in comparison with other drugs. The accelerated release time course observed in the VFS may simply be a function of the condensed nature of the model. The volume of bead suspension delivered is a tenth of what is used in the swine model, therefore delivery of the entire dose does not take as long, and the channels are blocked quickly as beads reach the filters, leading to the reduction of drug release. Another key difference is that since the VFS is a semi-open loop system, the drug concentration that is recorded at each time point provides a snapshot of what has been released in that moment, in other words the drug does not have the opportunity to accumulate as it would in the plasma prior to the start of elimination. Doxorubicin has a very short distribution half-life of 5 min (Drugbank, 2017), in other words it is quickly distributed into other bodily compartments which is reflected in its early disappearance from the plasma compared to irinotecan and vandetanib. This may be why a better correlation was achieved with doxorubicin in the VFS, where the eluted drug is also quickly removed from the system.

4.2.2. Flow through model

The flow through cell model employed in this study mimics packing of beads in blood vessels with a very slow flow rate, which makes it suitable for modelling the mid to late phase of drug release from DEB *i.e.* post-administration. A number of other drug elution methods have been described in the literature that attempt to model drug release over this phase, including a T-apparatus in which DEBs sit in a well and drug release controlled initially by diffusion in the well followed by more distant convection (Amyot et al., 2002). More recently, a USP Type IV flow-through system was described in which DEBs were placed on top of a column of glass beads that generate a laminar flow regime (Jordan et al., 2010). Each of these methods has its merits but also limitations in terms of practical use and by no means reflect the actual elution kinetics observed *in vivo*. The flow through system was capable of distinguishing between the three drug types, showing the same pattern as the *in vivo* data in terms of the relative release rate of irinotecan, vandetanib and doxorubicin as a consequence of drug binding strength, interactions, and solubility. A linear point-to-point correlation was achieved for the first 24 h when comparing the AUC derived from the flow through data and *in vivo* plasma data for vandetanib. The lack of correlation after 24 h was caused by the drug levels dropping significantly in the swine plasma whilst drug release *in vitro* continued. This is likely due to the onset of phase 3 drug release *in vivo*, where blood clotting and stasis has occurred and the beads are firmly embedded in an embolus. Drug diffuses out of the beads and now directly into the surrounding tissue, rather than directly into the blood circulation as can occur during the administration and redistribution phases. The presence of plasma proteins in blood may also contribute to differences in drug release rate *in vivo*, as adsorption of these proteins into PVA based biomaterials has been documented with unknown effects on drug release. The *in vitro* elution system therefore is not refined enough to be able to model this biological process. Doxorubicin and irinotecan had differential release rates in the flow through model compared to *in vivo*, and a point to point IVIVC was not even achieved for these drugs.

By convoluting *in vitro* elution data, it is possible to predict plasma concentrations by mathematical simulation of drug elimination. When this process was applied to our data, the convoluted *in vitro* profiles only showed similarities in elimination phase curve shape for vandetanib and irinotecan. In contrast to the VFS model, the predicted T_{max} were this time several hours later than the actual *in vivo* T_{max}. However, this

can be explained by the fact that the flow through elution process is started with the beads already in an occlusive mass, therefore the burst effect is not modelled and the drug will take longer to reach a peak concentration. FDA guidance states that time-scaling or time shift correction may be applied to the *in vitro* profile to improve the alignment (FDA, 1997), which has been successfully implemented in developing IVIVC in non-intravenous microsphere formulations using modified USP IV apparatus (Andhariya et al., 2017). Doxorubicin IVIVC was not improved by implementing a simple time shift correction to account for the slow initial release rate, therefore further investigation is required to establish if time-scaling may be appropriate. If the time-scaling factor is found to be non-linear, the lack of consistency between release rates should be treated as a limitation of the *in vitro* model.

Despite using the same volume of beads and drug doses as were used in the *in vivo* studies, the convoluted profile significantly underestimated the plasma concentrations of all three drugs, although the disparity decreases over time and the values begin to converge after 24 h–48 h. Again, this may be related to the lack of the burst phase and the tight packing and slow flow rate of the system. In particular, doxorubicin was initially very slow to elute from the beads in the flow through model, which may be due to how it is released when packed in a column. Swaine et al. (2016) found that dox release from DC Bead™ in a column was based on a process of drug desorption from the near end of the column, followed by resorption by beads further along in the direction of flow (Swaine et al., 2016). This results in the beads furthest away from the flow source becoming loaded with more drug than the initial loading dose, which may increase drug aggregation and impede ion influx. This effect has resulted in a slow, sustained release of dox in the flow through model, which offset the simulated elimination giving a shallower elimination curve in the convoluted data. *In vivo*, as previously mentioned dox is quickly distributed into tissues and this is not accounted for in the convolution process.

Convolution of *in vitro* data is one approach to develop an IVIVC, however the method used in this study is traditionally used for either oral or instantaneous i.v. dosage forms, which may mean it is not optimised for controlled release applications. Indeed, a further limitation of our pharmacokinetic studies was restriction of the number of blood samples that could be taken and hence lack of data points for correlation. Reported $T_{1/2}$ and V_d for the drugs were found to be variable in the literature, and values obtained for humans may not be applicable to swine. Therefore, apparent $T_{1/2}$ and V_d were obtained from the corresponding DEB pre-clinical studies where possible to improve accuracy. For LUMIDOX they could not be calculated and therefore the parameters were taken from a published study that used i.v. infusion of dox solution in swine rather than DEB, which may limit the accuracy of the prediction, as controlled release formulations can cause apparent $T_{1/2}$ and V_d to vary from the standard values. A possible alternative approach would be to de-convolute the *in vivo* data and compare this with the dissolution profiles.

5. Conclusions

The models described here have given an insight into how we may start to improve representativeness of *in vitro* elution testing for drug eluting beads. The early phase VFS model allowed an estimation of the proportion of drug that would be released during the administration phase of DEB-TACE, which can provide an indicator of the relative degree of systemic exposure for different drugs. Vandetanib burst release from LUMIVAN was within a similar range to commonly used drugs irinotecan and doxorubicin, therefore providing encouragement that systemic exposure will remain within acceptably low levels for this novel DEB. The flow through model, as intended, seemed more suited to modelling mid to late phase drug release as it did not predict the early burst effect, but instead corresponded better to the drug elimination phase. It seems that adapting and combining these two methods may offer an improved method of predicting plasma drug concentrations after DEB treatment. Looking forward, it will be of interest to develop a third model based on drug diffusion from DEB into a biomimetic matrix in order to model tissue diffusion, which will complete the picture of the fate of drugs released from embolic beads.

Acknowledgements

The authors would like to thank MPI Research for conducting the embolization procedures and pharmacokinetic analysis, Worldwide Clinical Trials for the plasma analysis of doxorubicin and irinotecan, and York Bioanalytical Solutions Limited for the plasma analysis of vandetanib. Biocompatibles UK Ltd. for access to the pharmacokinetic data for the correlation studies and permission to publish. A. Hagan would like to thank the Royal Commission for the Exhibition of 1851 for the provision of funding *via* an Industrial Fellowship.

Appendix A. Supplementary data

Supplementary data to this article can be found online at https://doi.org/10.1016/j.ejps.2019.05.021.

References

Ahnfelt, E., et al., 2016. In vitro release mechanisms of doxorubicin from a clinical bead drug-delivery system. J. Pharm. Sci. 105 (11), 3387–3398.
Ahnfelt, E., et al., 2018. Single bead investigation of a clinical drug delivery system – a novel release mechanism. J. Control. Release 292, 235–247.
Amyot, F., et al., 2002. A new experimental method for the evaluation of the release profiles of drug-loaded microbeads designed for embolisation. ITBM-RBM 23 (5), 285–289.
Andhariya, J.V., et al., 2017. Development of in vitro-in vivo correlation of parenteral naltrexone loaded polymeric microspheres. J. Control. Release 255, 27–35.
Ashrafi, K., et al., 2017. Characterization of a novel intrinsically radiopaque drug-eluting bead for image-guided therapy: DC bead LUMI™. J. Control. Release 250, 36–47.
Biondi, M., et al., 2013. Investigation of the mechanisms governing doxorubicin and irinotecan release from drug-eluting beads: mathematical modeling and experimental verification. J. Mater. Sci. Mater. Med. 24 (10), 2359–2370.
Boulin, M., et al., 2014. Idarubicin-loaded beads for chemoembolisation of hepatocellular carcinoma: results of the IDASPHERE phase I trial. Aliment. Pharmacol. Ther. 39 (11), 1301–1313.
Caine, M., 2017. Gel phantom for real-time in vitro spatiotemporal diffusion of doxorubicin from radiopaque and non-radiopaque drug eluting beads introduction. J. Vasc. Interv. Radiol. 28 (6), e47–e48.
Caine, M., et al., 2017a. Review of the development of methods for characterization of microspheres for use in embolotherapy: translating Bench to Cathlab. Adv. Healthc. Mater. 6 (9), 1601291.
Caine, M., et al., 2017b. Impact of yttrium-90 microsphere density, flow dynamics, and administration technique on spatial distribution: analysis using an in vitro model. J. Vasc. Interv. Radiol. 28 (2), 260–268.e2.
ClinicalTrials.gov, 2017. Vandetanib-eluting radiopaque embolic beads in patients with resectable liver malignancies (VEROnA). [cited 2018 19/01/2018]; Available from: https://clinicaltrials.gov/ct2/show/NCT03291379.
de Baere, T., et al., 2016. An in vitro evaluation of four types of drug-eluting microspheres loaded with doxorubicin. J. Vasc. Interv. Radiol. 27 (9), 1425–1431.
Denys, A., et al., 2017. Vandetanib-eluting radiopaque beads: in vivo pharmacokinetics, safety and toxicity evaluation following swine liver embolization. Theranostics 7 (8), 2164–2176.
Drugbank, 2017. Doxorubicin. [09/01/2018]; Available from: https://www.drugbank.ca/drugs/DB00997.
Dubbelboer, I.R., et al., 2014. The effects of lipiodol and cyclosporin A on the hepatobiliary disposition of doxorubicin in pigs. Mol. Pharm. 11 (4), 1301–1313.
Duran, R., et al., 2016. A novel inherently radiopaque bead for transarterial embolization to treat liver cancer - a pre-clinical study. Theranostics 6 (1), 28–39.
Facciorusso, A., 2018. Drug-eluting beads transarterial chemoembolization for hepatocellular carcinoma: current state of the art. World J. Gastroenterol. 24 (2), 161–169.
FDA, 1997. Guidance for Industry. Extended Release Oral Dosage Forms: Development, Evaluation, and Application of In Vitro/In Vivo Correlations.
Fuchs, K., et al., 2014. Drug-eluting beads loaded with antiangiogenic agents for chemoembolization: in vitro sunitinib loading and release and in vivo pharmacokinetics in an animal model. J. Vasc. Interv. Radiol. 25 (3), 379–387.
Fuchs, K., et al., 2015. Sunitinib-eluting beads for chemoembolization: methods for in vitro evaluation of drug release. Int. J. Pharm. 482 (1–2), 68–74.
Gonzalez, M.V., et al., 2008. Doxorubicin eluting beads-2: methods for evaluating drug elution and in-vitro:in-vivo correlation. J. Mater. Sci. Mater. Med. 19 (2), 767–775.
Gustafson, D.L., et al., 2002. Doxorubicin pharmacokinetics: macromolecule binding, metabolism, and excretion in the context of a physiologic model. J. Pharm. Sci. 91 (6), 1488–1501.
Hagan, A., et al., 2017. Preparation and characterisation of vandetanib-eluting radiopaque beads for locoregional treatment of hepatic malignancies. Eur. J. Pharm. Sci.

101, 22–30.
Jordan, O., et al., 2010. Comparative study of chemoembolization loadable beads: in vitro drug release and physical properties of DC bead and hepasphere loaded with doxorubicin and irinotecan. J. Vasc. Interv. Radiol. 21 (7), 1084–1090.
Lahti, S.J., et al., 2015. Sorafenib loaded drug-eluting beads: loading and eluting kinetics and in vitro viability study. J. Vasc. Interv. Radiol. 26 (2), S80–S81.
Lammer, J., et al., 2010. Prospective randomized study of doxorubicin-eluting-bead embolization in the treatment of hepatocellular carcinoma: results of the PRECISION V study. Cardiovasc. Intervent. Radiol. 33 (1), 41–52.
Lencioni, R., 2012. Chemoembolization for hepatocellular carcinoma. Semin. Oncol. 39 (4), 503–509.
Lewis, A.L., 2009. DC Bead™: a major development in the toolbox for the interventional oncologist. Expert Rev. Med. Devices 6 (4), 389–400.
Martin, R.C., et al., 2009. Transarterial chemoembolization of metastatic colorectal carcinoma with drug-eluting beads, irinotecan (DEBIRI): multi-institutional registry. J. Oncol. 2009, 539795.
Martin, R.C., et al., 2011. Hepatic intra-arterial injection of drug-eluting bead, irinotecan (DEBIRI) in unresectable colorectal liver metastases refractory to systemic chemotherapy: results of multi-institutional study. Ann. Surg. Oncol. 18 (1), 192–198.
Martin, R.C., et al., 2012. Optimal outcomes for liver-dominant metastatic breast cancer with transarterial chemoembolization with drug-eluting beads loaded with doxorubicin. Breast Cancer Res. Treat. 132 (2), 753–763.
Namur, J., et al., 2010. Drug-eluting beads for liver embolization: concentration of doxorubicin in tissue and in beads in a pig model. J. Vasc. Interv. Radiol. 21 (2), 259–267.
Nicolini, A., et al., 2010. Transarterial chemoembolization with epirubicin-eluting beads versus transarterial embolization before liver transplantation for hepatocellular carcinoma. J. Vasc. Interv. Radiol. 21 (3), 327–332.
Nicolini, A., Crespi, S., Martinetti, L., 2011. Drug delivery embolization systems: a physician's perspective. Expert Opin. Drug Deliv. 8 (8), 1071–1084.
Qureshi, S.A., 2010. In vitro-in vivo correlation (IVIVC) and determining drug concentrations in blood from dissolution testing - a simple and practical approach. Open Drug Delivery J. 4, 38–47.
Reich, S.D., et al., 1979. Mathematical model for adriamycin (doxorubicin) pharmacokinetics. Cancer Chemother. Pharmacol. 3 (2), 125–131.
Song, J.E., Kim, D.Y., 2017. Conventional vs drug-eluting beads transarterial chemoembolization for hepatocellular carcinoma. World J. Hepatol. 9 (18), 808–814.
Swaine, T., et al., 2016. Evaluation of ion exchange processes in drug-eluting embolization beads by use of an improved flow-through elution method. Eur. J. Pharm. Sci. 93, 351–359.
Taylor, R.R., et al., 2007. Irinotecan drug eluting beads for use in chemoembolization: in vitro and in vivo evaluation of drug release properties. Eur. J. Pharm. Sci. 30 (1), 7–14.